Theoretical Study on Non-Radiative Decay of Dimethylaminobenzonitrile Through Triplet State in Gas Phase, Non-Polar, and Polar Solutions.

Kayo Suda [†] *and Daisuke Yokogawa* [*, †, ‡]

† Department of Chemistry, Graduate School of Science, Nagoya University, Chikusa, Nagoya 464-8602, Japan
‡ Institute of Transformative Bio-Molecules (WPI-ITbM), Nagoya University, Chikusa, Nagoya 464-8602, Japan

AUTHOR INFORMATION

Corresponding Author

*E-mail: d.yokogawa@chem.nagoya-u.ac.jp

Abstract

In the design of bio-imaging molecules, the control of radiative and non-radiative decay is important. Dimethylaminobenzonitrile (DMABN) is a suitable model molecule to study radiative and non-radiative decay processes and has been investigated by theoretical and experimental methods. However, an atomistic understanding of non-radiative decay in solutions remains to be achieved. In this study, we investigated the potential energy surfaces in excited states along the rotation of the dimethylamino group and found that the degeneration between S_1 and T_1 states is one of the key factors in non-radiative decay in polar solvents. In addition, we found that the degeneration is precisely controlled by a fundamental physical property, exchange integral. Although DMABN is a simple molecule, the understanding of non-radiative decay process based on physical properties should be useful in the design of more complicated imaging molecules.

Introduction

Bio-imaging techniques using fluorescence spectroscopy and microscopy are powerful tools for investigating systems such as plant structures and hormones.[1] Recent bio-imaging techniques development is significant in combination with novel bio-imaging molecules.[2-8] The fluorescence molecules for the bio-imaging must have high quantum yield and it would be useful to be reflected by surrounding environment, such as polar and non-polar characteristics. Recently, not only fluorescence-radiative decay, but also non-radiative decay, are becoming important in bio-imaging molecules, such as biosensors that have on-off switching fluorescence characteristics.[9, 10] Nevertheless, the mechanism of non-radiative decay process is still under investigation because of its complication. To optimize the use of the non-radiative decay in bio-imaging molecules, it is significantly useful to understand the decay mechanism with fundamental physical-chemical properties.

In bio-imaging molecules, amino group is one of the most employed functional groups. By tuning of the donation strength, we can control the fluorescence color in solutions and many kinds of unique molecules have been proposed.[11-13] However, another important factor of amino group is not so focused on, to the best our knowledge. Amino group greatly affects non-radiative decay process. If we can elucidate the non-radiative decay process, the amino group should become a useful functional group that can highly functionalize the bio-imaging molecules.

In this study, to understand the non-radiative decay of amino-group, we picked up dimethylaminobenzonitrile (DMABN). DMABN is one of the simplest molecules which have amino group and has been investigated in experimental and theoretical studies,[14 - 41] because of the rotation of the dimethylamino group and the fact that its fluorescence in its excited state is affected by polar and non-polar solvents.[14] The structure of DMABN is indicated in

Scheme 1. It is well known that the radiative decay of DMABN in solution is affected by the rotation of the dimethylamino group, from previous experimental studies.[14, 26-29, 31, 37, 38] Although experimental research on DMABN in solution, studied by time-resolved fluorescence spectroscopy, has been performed to clarify this reaction on an ultrafast time scale specifically focused on the rotation of the dimethylamino group,[26-28] an understanding of the non-radiative decay process from the singlet state to another state has not been achieved because of quenching fluorescence. While in some studies with time-resolved absorption spectroscopy a chemical species appeared in the visible region after quenching fluorescence of DMABN in polar solution, this species was assigned as the triplet state of DMABN.[15, 17-20, 26, 28] In addition, this assignment was consistent with the results of time-resolved infrared spectroscopy in polar and non-polar solvents.[29] These two spectroscopy methods suggested that DMABN might have a transition from S_1 to T_1 states in polar solutions, although these results do not verify the atomistic characteristics of T_1 state of DMABN, which could not be shown by any spectroscopy methods. Even now, the decay process of DMABN in each type of solution is not understood clearly.

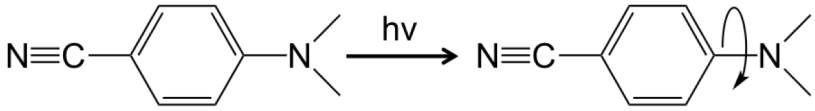

Scheme 1. Structure of DMABN.

In this article, to clarify the non-radiative process of DMABN in solution, we performed a calculation with quantum and statistical mechanics. In the most of previous theoretical studies, the non-radiative process was discussed by focusing on the transition from S_1 to S_0 states. Based on the previous experimental studies, we discussed the decay process from S_1 to T_1 states in polar and non-polar solvents. In the discussion, we aim to understand the mechanism using fundamental physical chemical properties, such as energy gap, orientation of lone pair orbital, exchange term, and so on.[42] Because these properties are not restricted to

DMABN, the knowledge obtained in this study will give us a fruitful hint to understand the non-radiative decay processes in other molecules that have amino groups.

Computational details

We performed optimization and energy calculations in gas and solution phases at the (TD) CAM-B3LYP/6-31+G(d) level of theory.[43] Dihedral angles (ω, ϕ, θ) are defined as ∠C3-C4-N2-C5, ∠C5-C4-N2-C7, and ∠C7-N2-C4-C8 as described in Scheme 2. All calculations were performed using the GAMESS program package.[44]

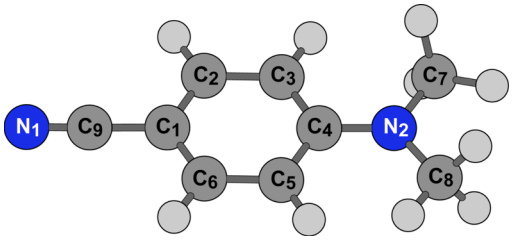

Scheme 2. Atomic labels of DMABN.

The solvation effect was computed with RISM-SCF-SEDD, which is one of the hybrid methods between quantum mechanics and statistical mechanics.[45-49] By computing solvation effect with distribution functions, we can perform the calculations in solution with reasonable computational cost. The RISM integral equation was coupled with the Kovalenko-Hirata closure.[50] The temperature was 300 K and the number density was 0.0153 for acetonitrile, 0.0148 for methanol, 0.0094 for dichloromethane, and 0.0055 molecules $Å^{-3}$ for cyclohexane. The Lennard-Jones parameters for

Table 1. Lennard-Jones parameters of DMABN.

Site	σ/ Å	ε/ kcal mol^{-1}
	Aromatic group	
C	3.550	0.070
H	2.420	0.030
	Cyano group	
C	3.650	0.150
N	3.200	0.170
	Dimethylamino group	
N	3.300	0.170
C	3.500	0.066
H	2.500	0.030

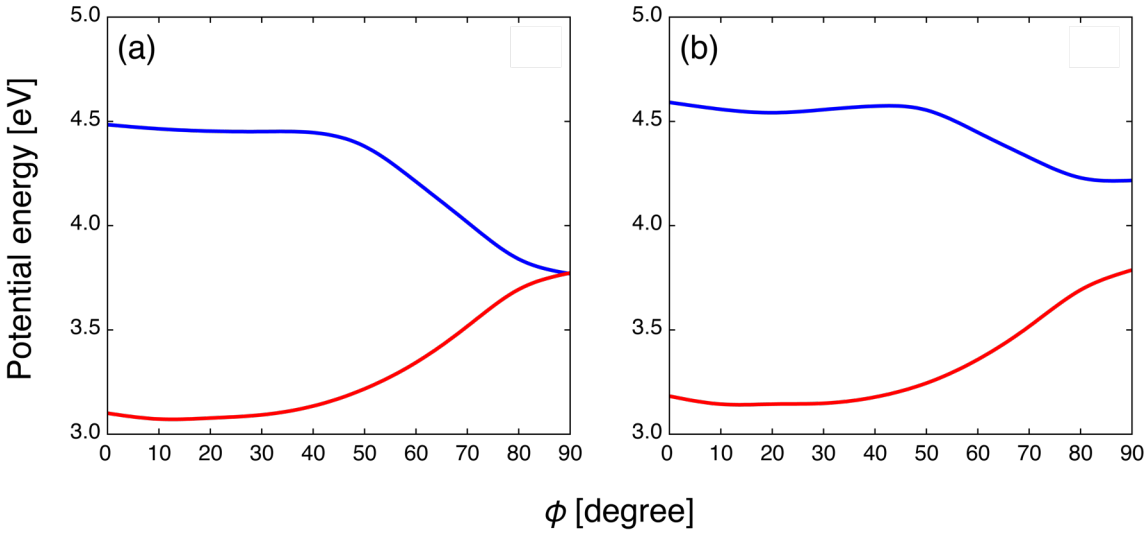

Figure 1. The potential energy surfaces of DMABN in S_1 state (blue line) and T_1 state (red line) in (a) acetonitrile and (b) gas phase along ϕ. The ground state (S_0) energy at $\phi = 0$ is set to zero.

the solute were determined based on OPLS-AA[51] and summarized in Table 1.

Results and Discussion

DMABN has been studied by many scientists, and it was shown that the rotation of the dimethylamino group is a key factor in radiative and non-radiative decays. To elucidate the importance of the rotation, we defined the three dihedral angles (ϕ, ω, θ) and constructed an energy surface in the gas phase at S_1 state (See Supporting Information). We found that the energy surface is mainly controlled by rotation of the dimethylamino group (ϕ) and wagging motions (ω, θ) do not change this characteristic. In the following discussion, we focused on the degree ϕ.

Figure 1 indicates the potential energy surfaces of DMABN at S_1 and T_1 states in acetonitrile and the gas phase along ϕ. The ground state energy at $\phi = 0$ is set to zero. When we compare the potential energy surfaces from $\phi = 0$ to 40 degrees at S_1 state for each phase, the free energy change is small in both the gas phase and acetonitrile. From $\phi = 50$ to 90 degrees, the free energy surfaces become stable in both cases. At $\phi = 90$ degrees, the

stabilization from $\phi = 0$ is 0.37 and 0.70 (eV) in the gas phase and acetonitrile, respectively. In the gas phase, DMABN can take both the rotated structure ($\phi = 90$) and the planar structure ($\phi = 0$) at room temperature because of the small energy change from $\phi = 0$ to 90 degrees, while it is not easy for DMABN to change to a planar structure from the rotated one in acetonitrile. In the case of T_1 state, the shape of the potential energy surface is similar in each phase. However, we found that there is a large difference in the energy gap between the gas phase and acetonitrile. S_1 and T_1 states become degenerate at 90 degrees in acetonitrile, while the energy gap is large 0.43 eV in the gas phase.

According to these results, it is found that the rotated structure ($\phi = 90$) should be a focus point to investigate the translation from S_1 to T_1 states. To discuss the energy gap between S_1 and T_1 states in several polar and non-polar solvents, we also performed the same calculations in methanol, dichloromethane, and cyclohexane. These results are summarized in Table 2. In methanol, protic polar solvent, the energy gap between S_1 and T_1 states at 90 degrees is small, as in the case of acetonitrile. On the basis of these results, we found that the degeneration between S_1 and T_1 states is not confined to acetonitrile. In dichloromethane, the degeneration could be obtained despite this being a non-polar solvent. In cyclohexane, however, the energy gap at 90 degrees between S_1 and T_1 states is large as in the case of the gas phase. This result shows that the polarity of dichloromethane is the threshold to determine whether DMABN has an energy gap between S_1 and T_1 states in the rotated structure. It was also found that the dependency of the fluorescence of DMABN on the solvent polarization could be explained by the difference in the decay processes, in particular the degenerative trend between S_1 and T_1 states. Non-radiative decay through T_1 state caused

Table 2. Energy gap between S_1 and T_1 states at 90 degrees in solutions (unit: eV).

	Acetonitrile	Methanol	Dichloromethane	Cyclohexane	Gas phase
Δ_{S-T}	0.00	-0.01	-0.01	0.42	0.43

by the degeneration is a critical occasion for low-intensity fluorescence in each polar solvent. In non-polar solvents, such as hexane, there is an energy gap between S_1 and T_1 states and the decay through T_1 state is suppressed because of the energy gap.

These results are consistent with previous experimental studies, such as time-resolved infrared spectroscopy study and transient absorption studies. M. Hashimoto and H. Hamaguchi reported the results of a study of DMABN by time-resolved infrared spectroscopy in polar (butanol) and non-polar (hexane) solvents.[29] This report focused on the cyano group stretching frequency, and there is a significant structural effect of in the polar solvent. In the non-polar solvent, however, only one transient species was detected. This indicated that the transition from S_1 and T_1 states in the rotated structure could exist in a polar solvent, but not in a non-polar solvent. Our result is certainly consistent with these results.

Before we discuss the origin of the energy gap in details, it would be important to check the reliability of our calculations based on TD-CAM-B3LYP. For this purpose, we employed Multi-Reference Møller-Plesset 2nd order (MR-MP2)[52] coupled with RISM. Because of the computational cost and the stability of the calculations, we computed S_1 and T_1 states with a medium size of basis set (cc-pVDZ) and treated with C_{2v} symmetry structure optimized at ϕ = 90 degree. It is well known that MR-MP2 is a powerful tool for

Table 3. Emission energy and energy gap Δ_{S-T} at ϕ = 90 degree in gas phase and acetonitrile computed with TD-DFT and MR-MP2 (unit: eV).

	Emission energy		Energy gap Δ_{S-T}	
	gas	acetonitrile	gas	acetonitrile
TD-DFT	3.47	2.48	0.36	0.00
MR-MP2	3.41	2.72	0.49	-0.01
exp.[a)]	3.66	2.52	-	-

a) Ref.[54]

investigating electronic structures of molecules and the excitation energies computed with MR-MP2 are quite good.[53] In Table 3, we summarized the emission energy and energy gap Δ_{S-T} at ϕ = 90 degree in gas phase and acetonitrile. About the emission energy, we also showed the experimental data. In emission energy, TD-DFT data reproduced the experimental data and MR-MP2 data in gas phase and acetonitrile. In the case of energy gap, we do not have experimental data and cannot compare TD-DFT data with experimental one. However, even in the case of MR-MP2, the energy gap Δ_{S-T} is not zero in gas phase, while the energy gap is negligible in acetonitrile, which is the same with TD-DFT results. From the data shown in Table 3, we can conclude that our TD-DFT data in this study are reliable.

Why are there some differences in the energy gap at 90 degrees between the gas phase and acetonitrile? First, we computed the electronic structure at 90 degree and found a charge difference between the planar and rotated structures at T_1 state, as shown in Figure 2(a). In acetonitrile, a nitrogen atom of the dimethylamino group (N2) has a positive charge difference, and some atoms of the benzene ring and cyano group have negative charge differences. This means that an electron is transferred from the lone pair of the nitrogen atom of the dimethylamino group to other atoms along the dihedral angle change, which is a typical charge-transfer (CT) characteristic. In the gas phase, the N2 group and the carbon connected to the nitrogen atom (C4) have the opposite charge difference compared with that in acetonitrile, which shows a π-π^* like character. The electronic structure difference at T_1 state between acetonitrile and gas phase can be also seen in the dipole moment. We show the dipole moment changes at S_1 and T_1 states in the gas phase and acetonitrile in Figure 2(b). The dipole moment at 90 degrees is drastically different between S_1 and T_1 states in the gas phase, while the dipole moment is almost the same in acetonitrile. In addition, the trends in the dipole moments at T_1 state are exactly the opposite to those between the gas phase and acetonitrile, despite those at S_1 state being similar for every rotation degree. From Figures 2

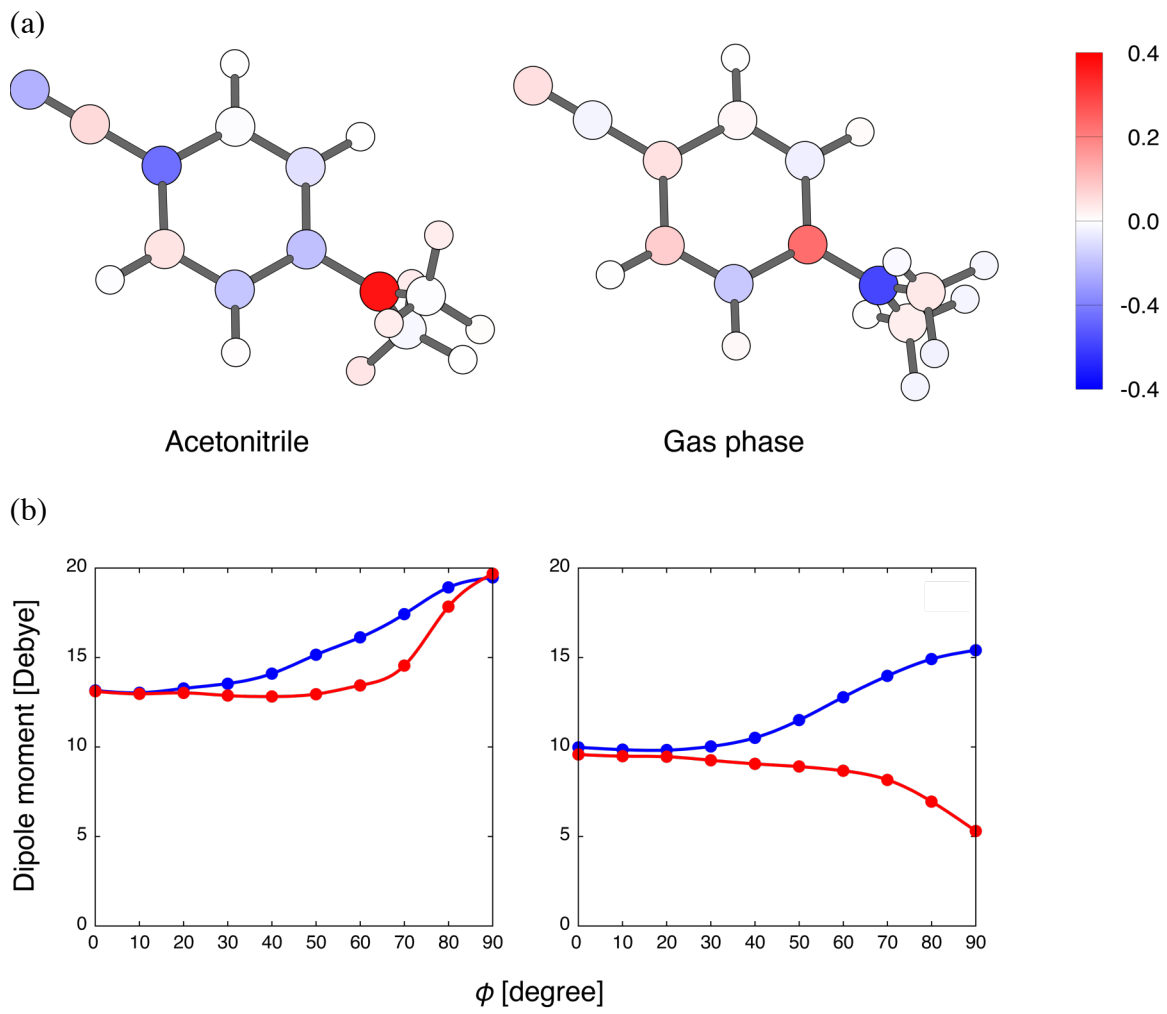

Figure 2. (a): The charge difference (Δq) of DMABN between planar and rotated structures at T_1 state. (b): The dipole moment of DMABN at S_1 state (blue) and T_1 state (red) in acetonitrile (left) and gas phase (right) along ϕ.

(a) and 2 (b), the difference in Δ_{S-T} should come from the excitation character (CT or π-π*) at T_1 state.

The difference in the excitation character at T_1 state can be discussed with molecular orbitals (MOs). In Figure 3, we showed MOs of DMABN at 90 degrees at S_1 and T_1 states in acetonitrile, gas phase, and cyclohexane. The orbitals are the beta orbital where the electron is removed (MO39) and the alpha orbital where the electron enters (MO40) at T_1 state, and natural orbitals (NOs) at S_1 state. In the case of the NOs, we also showed the occupation number. At first, we focused on S_1 state in each solution. The occupation number showed that

the one-electron transition from MO39 to MO40 is dominant for $S_0 \rightarrow S_1$ excitation. The MOs indicate lone pair and π* characteristics at MO39 and MO40, respectively, in each solvent. According to these results, $S_0 \rightarrow S_1$ is an n-π* transition (CT) and this character is not changed by the solvent. Secondly our focus is the difference between the MO at T_1 state in acetonitrile and that in gas phase. In acetonitrile, MOs at T_1 state are similar to NOs at S_1 state, which means that $S_0 \rightarrow T_1$ is an n-π* transition. On the contrary, the beta orbital where the electron is removed (MO39) in gas phase is π orbital, which means that $S_0 \rightarrow T_1$ is a π-π* transition. In the case of cyclohexane, which also has none zero energy gap, $S_0 \rightarrow T_1$ state is also a π-π* transition. From the MOs, the energy gap difference should be explained by the difference in the frontier orbitals (MO39 and MO40) at T_1 state.

The frontier orbital character plays an important role to determine the energy gap Δ_{S-T}.[42] In our case, Δ_{S-T} can be computed with the exchange integral, K, as follows;

$$\Delta_{S\text{-}T} \sim 2K(\mathrm{MO39,MO40}), \quad (1)$$

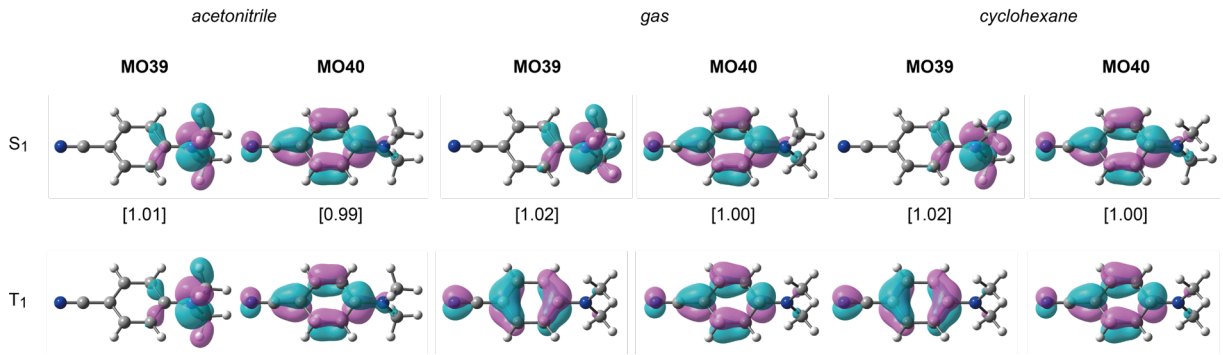

Figure 3. Molecular orbitals of DMABN in S_1 and T_1 states at 90 degrees in acetonitrile, gas phase, and cyclohexane. In the case of S_1 state, natural orbitals are shown and the occupation numbers of the natural orbitals are given in parenthesis. For T_1 state, the beta orbital where the electron is removed (MO39) and the alpha orbital where the electron enters (MO40) are shown.

$$K(\mathrm{MO39, MO40}) = \iint \psi_{39}(\mathbf{r}_1)\psi_{40}(\mathbf{r}_2)\left(\frac{1}{|\mathbf{r}_1-\mathbf{r}_2|}\right)\psi_{39}(\mathbf{r}_2)\psi_{40}(\mathbf{r}_1)d\mathbf{r}_1 d\mathbf{r}_2. \quad (2)$$

In Eq (1), we assumed that doubly occupied orbitals except for MO39 and MO40 are the same for S_1 and T_1 states. When the orbitals (ψ_{39} and ψ_{40}) do not overlap significantly, K becomes also small, as does the energy gap between S_1 and T_1 states.[42] In the case of gas phase (and cyclohexane), MO39 and MO40 are π and π* orbitals, respectively, while MO39 is lone pair orbital in the case of acetonitrile. Because the lone pair and π* orbitals are localized, K for acetonitrile is small and S_1 and T_1 states are degenerate.

We summarized the energy scheme in Scheme 3 based on the above discussions. In a polar solvent, the π-π* state at S_1 and T_1 states is unstable compared to the n-π* state. As described in this energy scheme, $2K$ does not change the relative stabilities between the n-π* and π-π* states because n-π* is greatly stabilized by the solvation effect. Therefore, Δ_{S-T} becomes negligible and the non-radiative process from S_1 to T_1 states occurs through the n-π* state. On the other hand, in the case of a non-polar solvent, stabilization of the n-π* state is small and $2K$ affects the energy inversion between the n-π* and π-π* states at T_1 state. Because there is an energy gap between n-π* at S_1 state and the π-π* state at T_1 state, the non-radiative process does not occur in non-polar solvents.

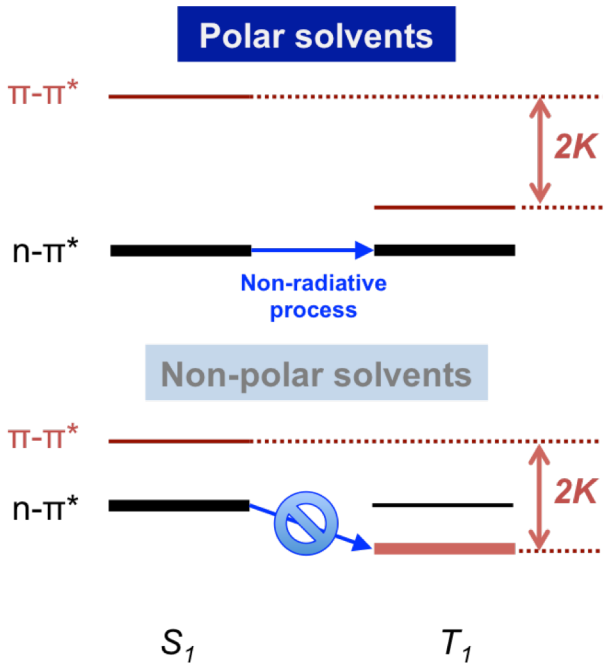

Scheme 3. Energy scheme for DMABN in S_1 and T_1 states in polar and non-polar solvents. The bold line indicates the state we obtained in this calculation.

Scheme 3 clearly shows that the non-radiative decay process is controlled by the solvent polarity. However, to understand the non-radiative process in solution specifically, we also have to evaluate the reorganization energy of the solvent. If the reorganization energy is large, the transition rate should become small. To discuss the reorganization energy, we computed the solvation structure. Figure 4 indicates the radial distribution functions (RDFs) of (a) nitrogen atoms of the cyano group of DMABN - methyl group of acetonitrile and (b) the nitrogen atom of the dimethyl amino group – methyl group of acetonitrile, at 90 degrees for the dimethylamino group at S_1 and T_1 states. As indicated in Figure 4(a), the RDFs at S_1 and T_1 states are almost the same, and a peak around 4 Å is so sharp that this interaction is somewhat tight. On the other hand, no significant peak exists in Figure 4(b), and there is no difference in the RDFs between the S_1 and T_1 states, as in Figure 4(a). These results indicate that the solvation structures at 90 degrees are almost the same for S_1 and T_1 states, and the reorganization energy of acetonitrile at 90 degree is small. Because of the small reorganization energy, S_1 to T_1 transition is possible in the case of acetonitrile.

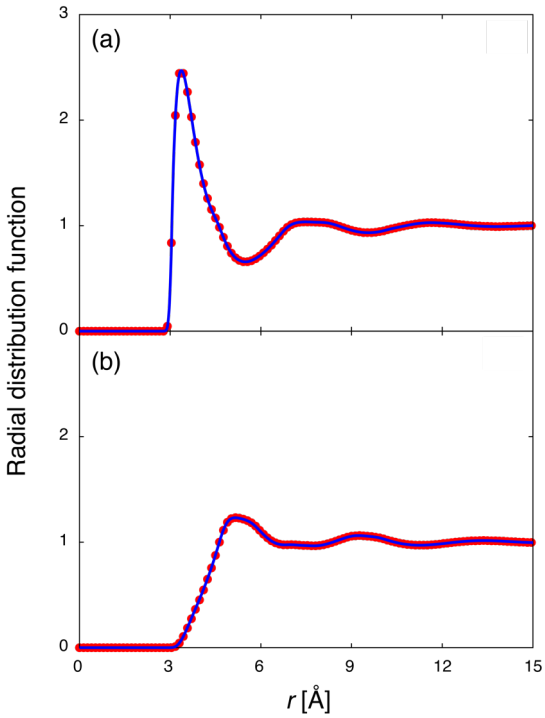

Figure 4. Radial distribution functions of DMABN in acetonitrile between methyl group of acetonitrile and (a) the nitrogen atom of the cyano group of DMABN, and (b) the nitrogen atom of the dimethyl amino group. The data for S_1 and T_1 states are shown with a solid line and filled circles, respectively.

Conclusions

We successfully revealed the non-radiative decay of DMABN through T_1 state in the gas phase, and in non-polar, and polar solutions, based on theoretical methods. The potential energy surface of DMABN at S_1 and T_1 states in the gas phase and acetonitrile showed that the degeneration between S_1 and T_1 states at 90 degrees in acetonitrile could occur, but not in the gas phase. We also calculated the energy at 90 degrees in some other solvents and found that the degeneration could occur in polar solvents, but not in non-polar solvents, such as cyclohexane. To discuss why there is a difference in the energy surfaces in these solvents, we focused on the electronic structures. The differences in atomic charges and dipole moment of DMABN indicated that there are CT and π-π^* characteristics in acetonitrile and the gas phase, respectively, at T_1 state. The analysis of the frontier orbitals showed that T_1 state in acetonitrile is expressed with n-π^* transition, while T_1 state is expressed with π-π^* transition in gas phase (and cyclohexane). By considering exchange integral, we found that the energy gap difference between acetonitrile and gas phase is caused by the overlap between the frontier orbitals. We also checked reorganization energy of solvent by computing RDFs and showed that the reorganization energy of acetonitrile is small. According to this analysis, it is found that the non-radiative process from S_1 to T_1 states could occur in polar solvents, but not in non-polar solvents.

We clearly showed that the balance between solvent-polarity and the relative stabilities between the n-π^* and π-π^* states play a key role in the non-radiative decay of DMABN. In this study, we obtained the results by employing simple physical chemical properties, such as exchange integral, orbital character difference, and so on. Because these properties are not restricted to DMABN, we can utilize the knowledge to bio-imaging molecules that have amino groups. If we can tune the balance by introducing functional groups, we can prepare

not only bright dyes, but also switching dyes. This study is useful not only from a physical chemistry viewpoint but also for the design of bio-imaging molecules.

Supporting Information.

We performed the calculation of potential energy surface of DMABN at S_1 state in gas phase containing wagging motions (ω, θ).

AUTHOR INFORMATION

Notes

The authors declare no competing financial interests.

Acknowledgement

This work was supported by the Grand-in-Aid for Scientific Research (C) (No.15K05385).

REFERENCES

(1) Tsuchiya, Y.; Yoshimura, M.; Sato, Y.; Kuwata, K.; Toh, S.; Hoibrook-Smith, D.; Zhang, H.; McCourt, P.; Itami, K.; Kinoshita, T.; Hagiwara, S. Probing Strigolactone Receptors in *Striga Hermonthica* with Fluorescence. *Science*. **2015**, *349*, 864-868.

(2) Fujikawa, Y.; Urano, Y.; Komatsu, T.; Hanaoka, K.; Kojima, H.; Terai, T.; Inoue, H.; Nagao, T. Design of Synthesis of Highly Sensitive Fluorogenic Substrates for Glutathione S-Transferase and Application for Activity Imaging in Living Cells. *J. Am. Chem. Soc.* **2008**, *130*, 14533-14543.

(3) Kobayashi, T.; Komatsu, T.; Kamiya, M.; Campos, C.; Gonz**á**lez-Gait**á**n, M.; Terai, T.; Hanaoka, K.; Nagao, T.; Urano, Y. Highly Activatable and Environment-Intensitive Optical Highlighters for Selective Spatiotemporal Imaging of Target Proteins. *J. Am. Chem. Soc.* **2011**, *134*, 11153-11160.

(4) Wang, C.; Fukazawa, A.; Taki, M.; Sato, Y.; Higashiyama, T.; Yamaguchi, S. A Phosphole Oxide Based Fluorescent Dye with Exceptional Resistance to Photobleaching: A Practical Tool for Continuous Imaging in STED Microscopy. *Angew. Chem. Int. Ed.* **2015**, *54*, 15213-15217.

(5) Betzig, E. Single Molecules, Cells, and Super-Resolution Optics (Nobel Lecture). *Angew. Chem. Int. Ed.* **2015**, *54*, 8034-8053.

(6) Betzig, E. Single-Molecule Spectroscopy, Imaging, and Photocontrol: Foundations for Super-Resolution Microscopy (Nobel Lecture). *Angew. Chem. Int. Ed.* **2015**, *54*, 8067-8093.

(7) Chen, W.; Pacheco, A.; Takano, Y.; Day, J, J.; Hanaoka, K.; Xian, M. A Single Fluorescent Probe to Visualize Hydrogen Sulfide and Hydrogen Polysulfides with Different Fluorescence Signals. *Angew. Chem. Int. Ed.* **2016**, *55*, 9993-9996.

(8) Uno, K.; Sasaki, T.; Sugimoto, N.; Ito, H.; Nishihara, T.; Hagihara, S.; Higashiyama, T.; Sasaki, N.; Sato, Y.; Itami, K. Key Structural Elements of Unsymmetrical Cyanine Dyes for Highly Sensitive Fluorescence Turn-On DNA Probes. *Chem. Asian J*. **2017**, *12*, 233-238.

(9) Usui, K.; Ando, M.; Yokogawa, D.; Irle, S. Understanding the On-Off Switching Mechanism in Cationic Tetravalent Group-V-Based Fluoride Molecular Sensors Using Orbital Analysis. *J. Phys. Chem. B*. **2015**, *119*, 12693-12698.

(10) Usui, K.; Irle, S.; Yokogawa, D. Understanding of the Off-On Response Mechanism in Caged Fluorophores Based on Quantum and Statistical Mechanics. *J. Phys. Chem. B*. **2016**, *120*, 4449-4456.

(11) Vendrell, M.; Zhai, D.; Er, J, C.; Chang, Y-T. Combinatorial Strategies in Fluorescent Probe Development. *Chem. Rev*. **2012**, *112*, 4391-4420.

(12) Yang, Y.; Zhao, Q.; Feng, W.; Li, F. Luminescent Chemodosimeters for Bioimaging. *Chem. Rev*. **2013**, *113*, 192-270.

(13) Singha, S.; Kim, D.; Roy, B.; Sanbasivan, S.; Moon, H.; Rao, A, S.; Kim, J, Y.; Joo, T.; Park, J, W.; Rhee, Y, M.; Wang, T.; Kim, K, H.; Shin, Y, H.; Jung, J.; Ahn, K, H. A Structural Remedy Toward Bright Dipolar Fluorophores in Aqueous Media. *Chem. Sci.,* **2015**, *6*, 4335-4342.

(14) Grabowski, Z, R.; Rotkiewicz, K.; Retting, W. Structual Changes Accompanying Intermolecular Electron Transter: Focus on Twisted Intramolecular Charge-Transfer States and Structures. *Chem. Rev*. **2003**, *103*, 3899-4031.

(15) Könler, G.; Granbner, G.; Rotkiewicz, K. Nonradiative Deactivation and Triplet States Donor-Aryl-Acceptor Compounds (Dialkylaminobenzonitrile). *Chem. Phys.* **1993**, *173*, 275-290.

(16) Nitin, C.; Rommens, J.; Auweraer, M, V, der A.; Schryver, Frans C. D. Laser-induced Optoacoustic Studies of the Non-Radiative Deactivation of ICT Probes DMABN and DMABA. *Chem. Phys. Lett.* **1997**, *264*, 265-272.

(17) Okada, T.; Uesugi, M.; Könler, G.; Rechthaler, K.; Rotkiewicz, K.; Retting, W.; Grabner, G. Time-Resolved Spectroscopy of DMABN and Its Cage Derivatives 6-Cyanobenzquinuclidine (CBQ) and Benzquinuclidine (BQ). *Chem. Phys.* **1998**, *241*, 327-337.

(18) Ma, C.; Kwok, W, M.; Matousek, P.; Parker, A. W.; Phillips, D.; Toner, W, T.; Towrie, M. Time-Resolved Study of the Triplet State of 4-Dimethylaminobenzonitrile (DMABN). *J. Phys. Chem. A.* **2001**, *105*, 4648-4652.

(19) Ma, C.; Kwok, W, M.; Matousek, P.; Parker, A. W.; Phillips, D.; Toner, W, T.; Towrie, M. Resonance Raman Study of Ring Deuterated 4-Dimethylaminobenzonitrile (DMABN-d4): the Ground, ICT and Triplet States. *J. Photochem. Photobio A: Chemistry*. **2001**, *142*, 177-185.

(20) Druzhinin, S, I.; Ernsting, N, P.; Kovalenko, S, A.; Lustres, L, P.; Senyushkina, T, A.; Zachariasse, K, A. Dynamics of Ultrafast Intramolecular Charge Transfer with 4-(Dimethylamino)benzonitrile in acetonitrile. *J. Phys. Chem. A.* **2006**, *110*, 2955-2969.

(21) Mennucci, B.; Toniolo, A.; Tomasi, J. Ab Initio Study of the Electronic Excited States in 4-(*N, N*-Dimethylamino)benzonitrile with Inclusion of Solvent Effects: The Internal Charge Transfer Process. *J. Am. Chem. Soc.* **2000**, *122*, 10621-10630.

(22) Cammi, R.; Mennucci, B.; Tomasi, J. Fast Evaluation of Geometries and Properties of Excited Molecules in Solution: A Tamm-Dancoff Model with Application to 4-Dimethylaminobenzonitrile. *J. Phys. Chem. A.* **2000**, *104*, 5631-5657.

(23) Xu, X.; Cao, Z.; Zhang, Q. Theoretical Study of Photoinduced Singlet and Triplet Excited States of 4-Dimethylaminobenzonitrile and Its Derivatives. *J. Chem. Phys.* **2005**, *122*, 194305.

(24) Chiba, M.; Tsuneda, T.; Hirao, K. Long-Range Corrected Time-Dependent Density Functional Study on Fluorescence of 4, 4'-Dimethylaminobenzonitrile. *J. Chem. Phys.* **2007**, *126*, 034504.

(25) Georgieva, I.; Aquino, A, J, A.; Plasser, F.; Trendafilova, N.; Köhn, A.; Lischka, H. Intramolecular Charge-Transfer Excited-State Processes in 4-(*N, N*-Dimethylamino)benzonitrile: The Role of Twisting and the πσ* State. *J. Phys. Chem. A.* **2015**, *119*, 6232-6243.

(26) Gustavsson, T.; Coto, P, B.; Serrano-Andrés, L.; Fujiwara, T.; Lim, E, C. Do Fluorescence and Transient Absorption Probe the Same Intramolecular Charge Transfer State of 4-(Dimethylaminobenzonitrile)?. *J. Chem. Phys.* **2009**, *131*, 031101.

(27) Fujiwara, T.; Zgierski, M, Z.; Lim, E, C. The Role of the πσ* State in Intramolecular Charge Transfer of 4-(Dimethylaminobenzonitrile). *Phys. Chem. Chem. Phys.* **2011**, *13*, 6779-6783.

(28) Coto, P. B.; Serrano-Andrés, L.; Gustavsson, T.; Fujiwara, T.; Lim, E, C. Intramolecular Charge Transfer and Dual Fluorescence of 4-(Dimethylaminobenzonitrile): Ultrafast Branching Followed by a Two-Fold Decay Mechanism. *Phys. Chem. Chem. Phys.* **2011**, *13*, 15182-15188.

(29) Hashimoto, M.; Hamagushi, H. Structure of the Twisted-Intramolecular-Charge-Transfer Excited Singlet and Triplet States of 4-(Dimethylaminobenzonitrile) As Studied by Nanosecond Time-Resolved Infrared Spectroscopy. *J. Phys. Chem.* **1995**, *99*, 7875-7877.

(30) Kajimoto, O.; Yokoyama, H.; Ooshima, Y.; Endo, Y. The Structure of 4-(*N*, *N*-Dimethylamino)benzonitrile and Its van der Waals Complexes. *Chem. Phys. Lett.* **1991**, *179*, 455-459.

(31) Baumann, W.; Bischof, H.; Fröhling, J.-C.; Brittinger, C.; Considerations on the Dipole Moment of Molecules Forming the Twisted Intramolecular Charge Transfer State. *J. Photochem. Photobiol. A: Chem.,* **1992**, *64*, 49-72.

(32) Schuddeboom, W.; Jonker, S, A.; Warman, J, M.; Leinhos, U.; Kühnle, W.; Zachariasse, K, A. Excited-State Dipole Moments of Dual Fluorescent 4-(Dialkylamino)benzonitrile. Influence of Alkyl Chain Length and Effective Solvent Polarity. *J. Phys. Chem.* **1992**, *96*, 10809-10819.

(33) Hayashi, S.; Ando, K.; Kato, S. Reaction Dynamics of Charge-Transfer State Formation of 4-(*N*, *N*-Dimethylamino)benzonitrile in a Methanol Solution: Theoretical Analyses. *J. Phys. Chem.* **1995**, *99*, 955-964.

(34) Il'ichev,Y.; Kühnle, W.; Zachariasse, K, A. Intramolecular Charge Transfer in Dual Fluorescent 4-(Dialkylamino)benzonitrile. Reaction Efficiency Enhancement by Increasing the Size of the Amino and Benzonitrile. *J. Phys. Chem. A.* **1998**, *102*, 5670-5680.

(35) Chudoba, C.; Kummrow, A.; Dreyer, J.; Stenger, J.; Nibbering, E, T, J.; Elsaesser, T.; Zachariasse, K, A. Excited State Structure of 4-(Dimethylamino)benzonitrile Studied by Femtosecond Mid-Infrared Spectroscopy and Ab initio Calculations. *Chem. Phys. Lett.* **1991**, *179*, 455-459.

(36) Rappoport, D.; Furche, F. Photoinduced Intramolecular Charge Transfer in 4-(dimethylamino)benzonitrile – A Theoretical Perspective. *J. Am. Chem. Soc.* **2004**, *126*, 1277-1284.

(37) Haidekker, M, A.; Brady, T, P.; Lichlyter, D.; Theodorakis, E, A. Effect of Solvent Polarity and Solvent Viscosity on the Fluorescent Properties of Molecular Rotors and Related Probes. *Bioorganic Chemistry*. **2005**, *33*, 415-425.

(38) Santhosh, K.; Banerjee, S.; Rangaraj, N.; Samanta, A. Fluorescence Response of 4-(*N, N'*-Dimerthylamino)benzonitrile in Room Temperature Ionic Liquids: Observation of Photobleaching under Mild Excitation Condition and Multiphoton Confocal Microscope Study of the Fluorescence Recovery Dynamics. *J. Phys. Chem. B.* **2010**, *114*, 1967-1974.

(39) Kochman, M, A.; Tajti, A.; Morrison, C, A.; Miller, R, J, D. Early Events in the Nonadiabatic Relaxation Dynamics of 4-(*N, N*-Dimethylamino)benzonitrile. *J. Chem. Theory Comput.* **2015**, *11*, 1118-1128.

(40) Gómez, I.; Castro, P, J.; Reguero, M. Insight into the Mechanism of Luminescence of Aminobenzonitrile and Dimethylaminobenzonitrile in Polar Solvents. An ab initio Study. *J. Phys. Chem. A.* **2015**, *119*, 1983-1995.

(41) Zhong, C. The Driving Forces for Twisted or Planar Intramolecular Charge Transfer. *Phys. Chem. Chem. Phys.* **2015**, *17*, 9248-9257.

(42) Turro, N, J. *Modern Molecular Photochemistry*. University Science Books. **1991**.

(43) Yanai, T.; Tew, D. P.; Handy, N. C. A New Hybrid Exchange–Correlation Functional Using the Coulomb-Attenuating Method (CAM-B3LYP). *Chem. Phys. Lett.* **2004**, *393*, 51-57.

(44) Schmidt, M. W.; Baldridge, K. K.; Boatz, J. A.; Elbert, S. T.; Gordon, M. S.; Jensen, J. H.; Koseki, S.; Matsunaga, N.; Nguyen, K. A.; Su, S.; Windus, T. L.; Dupuis, M.; Montgomery, J. A. General Atomic and Molecular Electronic Structure System. *J. Comput. Chem.* **1993**, *14*, 1347–1363.

(45) Hirata, F.; Rossky, P. J. An Extended RISM Equation for Molecular Polar Fluids. *Chem. Phys. Lett.* **1981**, *83*, 329-334.

(46) Ten-no, S.; Hirata, F.; Kato, S. A Hybrid Approach for the Solvent Effect on the Electronic-Structure of a Solute Based on the RISM and Hartree-Fock Equations. *Chem. Phys. Lett.* **1993**, *214*, 391-396.

(47) Sato, H.; Hirata, F.; Kato, S. Analytical Energy Gradient for the Reference Interaction Site Model Multiconfigurational Self-Consistent-Field Method: Application to 1,2-Difluoroethylene in Aqueous Solution. *J. Chem. Phys.* **1996**, *105*, 1546-1551.

(48) Yokogawa, D.; Sato, H.; Shigeyoshi, S. New Evaluation of Reconstructed Spatial Distribution Function from Radial Distribution Functions. *J. Chem. Phys.* **2007**, *126*, 244504.

(49) Yokogawa, D. New Fitting Approach of Electrostatic Potential for Stable Quantum Mechanical Calculations Using the Reference Interaction Site Model. *Chem. Phys. Lett.* **2013**, *587*, 113-117.

(50) Kovalenko, A.; Hirata, F. Self-Consistent Description of a Metal-Water Interface by the Kohn-Sham Density Functional Theory and the Three-Dimensional Reference Interaction Site Model. *J. Chem. Phys.* **1999**, *110*, 10095-10112.

(51) Jorgensen, W. L.; Maxwell, D. S.; Tirado-rives, J. Development and Testing of the OPLS All-Atom Force Field on Conformational Energetics and Properties of Organic Liquids. *J. Am. Chem. Soc.* **1996**, *118*, 11225-11236.

(52) Hirao, K. Multireference Møller-Plesset Method. *Chem. Phys. Lett.* **1992**, *190*, 374-380.

(53) *Recent Advances in Multireference Methods*; Hirao, K., Ed.; World Scientific: River Edge, NJ, 1999.

(54) Köhler, G.; Wolschann, P.; Rotkiewicz, K. Solvent Effects on Intramolecular Charge Separation. *Proc. Indian Acad. Sci. (Chem. Sci.)* **1992**, 104, 197-207.